Proceedings of the Steklov Institute of Mathematics, Suppl. 1, 2003, pp. S98–S107.
Translated from Trudy Instituta Matematiki i Mekhaniki UrO RAN, Vol. 9, No. 1, 2003.

Dispersion-managed Solitons in the Limit of Large Energy [1]

Henrik Kalisch[2] and Dmitry Pelinovsky[2]

Received November 11, 2002

Abstract—We study a dynamical system for Gaussian dispersion-managed pulses in the limit of large pulse energy and map strength. We show numerically and asymptotically that the pulse energy E grows with the map strength S as $E \sim D_+\sqrt{S}$, where D_+ is the effective dispersion coefficient of the focusing fiber. We also inspect leading-order asymptotic solutions that describe variations of the pulse parameters along the optical fiber.

1. INTRODUCTION

Return-to-zero pulses and dispersion-managed solitons are two elements in the endeavor to achieve higher bit rates for long-haul data transmission in dispersion-compensated optical fibers [4]. Dispersion-managed solitons can be modeled by special solutions of the periodic nonlinear Schrödinger equation [7]. An accurate approximation of dispersion-managed solitons is achieved with Gaussian pulses that are localized in time and vary periodically in distance along the optical fiber [3]. The Gaussian pulses are parametrized by the pulse energy, or, equivalently, by the map strength of the dispersion variations [8].

We have recently studied Gaussian pulses that approximate dispersion-managed solitons in the limit of short dispersion maps, when normal-form transformations can be applied for averaging the periodic nonlinear Schrödinger equation [6]. Here we study properties of the Gaussian pulses in the limit of large pulse energy and map strength, which is the opposite limit to the one in [6]. In optical communications, pulses of large energy are preferred because of a favorable signal-to-noise ratio, while strongly dispersion-managed maps reduce the four-wave mixing and improve the bit rates of communication channels in the fiber bandwidth. In this context, we show that the pulse energy E grows with larger map strength S as $E \sim D_+\sqrt{S}$, where D_+ is the effective dispersion coefficient of the focusing fiber. This main result is derived by means of asymptotic analysis and is confirmed by direct numerical simulations.

2. MODEL

Transmission of optical pulses in a dispersion-managed optical fiber is modeled by the periodic nonlinear Schrödinger (NLS) equation,

$$iu_z + d(z)u_{tt} + \gamma(z)\,|u|^2\,u = 0, \tag{2.1}$$

[1] This article was submitted by the authors in English

[2] Department of Mathematics, McMaster University
1280 Main Street West, Hamilton, Ontario, Canada L8S 4K1

where $d(z)$ is a periodic dispersion coefficient and $\gamma(z)$ is a nonlinearity coefficient, modified due to fiber loss and amplification [8]. The dispersion map period and variance can be normalized by a simple scaling transformation [6], such that the dispersion map $d(z)$ takes the form

$$\begin{aligned} d(z) &= d_0 + d_+, \quad n < z < n + l, \\ d(z) &= d_0 + d_-, \quad n + l < z < n + 1, \qquad n \in \mathbb{Z}, \end{aligned} \tag{2.2}$$

where l is the length of the focusing fiber such that $0 < l < 1$, d_0 is the average dispersion, and $d_+ = 2/l$ and $d_- = -2/(1-l)$ are zero-mean variations of the dispersion coefficients in the focusing and defocusing fibers. In the same normalization, the nonlinearity coefficient $\gamma(z)$ takes the form

$$\gamma(z) = Ke^{-2\alpha(z-n-1)}, \qquad n + z_a \le z \le n + 1 + z_a, \qquad n \in \mathbb{Z}, \tag{2.3}$$

where $\alpha > 0$ is the decay rate due to fiber losses, z_a is a position of an amplifier in the dispersion map such that $0 \le z_a \le 1$, and K is a constant that normalizes the mean of the coefficient $\gamma(z)$ to one,

$$K = \frac{2\alpha e^{2\alpha z_a}}{e^{2\alpha} - 1}.$$

Dispersion-managed solitons are approximated by the Gaussian pulses in the following form:

$$u(z,t) = c\, \exp\Big(-\frac{t^2}{a - ib} + i\phi \Big), \tag{2.4}$$

where $a(z)$, $b(z)$, $c(z)$, and $\phi(z)$ are parameters of the Gaussian pulses varying with the distance along the fiber. The amplitude $c(z)$ follows from the power balance equation as

$$c = \frac{Ea^{1/2}}{\sqrt{2}(a + ib)},$$

where E is the energy of the Gaussian pulse. The width $a(z)$ and the chirp $b(z)$ satisfy the dynamical system

$$\begin{cases} \dfrac{da}{dz} &= \dfrac{E\gamma(z)a^{5/2}b}{(a^2+b^2)^{3/2}}, \\ \dfrac{db}{dz} &= d(z) - \dfrac{E\gamma(z)a^{3/2}(a^2-b^2)}{2(a^2+b^2)^{3/2}}, \end{cases} \tag{2.5}$$

and the phase shift parameter $\phi(z)$ is decoupled from the system with the separate equation

$$\frac{d\phi}{dz} = \frac{E\gamma(z)a^{1/2}(3a^2+5b^2)}{8(a^2+b^2)^{3/2}}. \tag{2.6}$$

The map strength S of the dispersion map is defined by the minimal values of $a(z)$ on a period $0 \le z \le 1$:

$$S = \frac{1}{\min\limits_{0 \le z \le 1} a(z)}. \tag{2.7}$$

From (2.4) and (2.5) it is clear that $b(z_0) = 0$ if z_0 is a minimum of $a(z)$ and that the map strength S is inverse proportional to the minimal pulse width [6].

Dispersion-managed solitons are described by the Gaussian pulses (2.4), computed at a periodic solution of the system (2.5) such that $a(z+1) = a(z)$, $b(z+1) = b(z)$, and $\phi(z+1) = \phi(z) + M$, where

M depends on E and S [6]. The existence of periodic solutions in the system (2.5) is rigorously proved in [2, 1]. Numerical simulations in [3, 7] confirm that the Gaussian pulses accurately approximate dispersion-managed solitons in the periodic NLS equation. It is shown in [5] that, for a positive average dispersion $d_0 > 0$, the system (2.5) has a stable elliptic fixed point in the Poincaré section of the periodic solutions (a, b), whereas for a negative average dispersion $d_0 < 0$, the system has a stable elliptic and an unstable hyperbolic fixed point. The averaging method is developed in [6] with a rigorous proof of stability–instability and bifurcations of different periodic solutions of the system (2.5). Here we study asymptotic properties of the system (2.5) in the limit of large E and S for either sign of d_0.

3. ASYMPTOTIC AND NUMERICAL RESULTS

We first find a numerical approximation of periodic solutions of system (2.5). We use a two-dimensional shooting method, where the Jacobian matrix is approximated by a first-order finite-difference operator at each time step. This algorithm does not always converge, but satisfactory convergence is found in most cases. Iterations are started with a reasonable initial approximation for $a(0)$ and $b(0)$, most often stemming from the approximation obtained for slightly different parameters E and S. To integrate the system (2.5) with given initial data, a four-step Runge-Kutta method is employed. Figure 1 shows the numerical approximation of the periodic solutions $a(z)$ and $b(z)$, the dispersion map $d(z)$ on $0 < z < 1$, and the phase plane (a, b) in the case when $l = 0.1$, $d_0 = 0.04$, $\alpha = 0$, and $E = 100$.

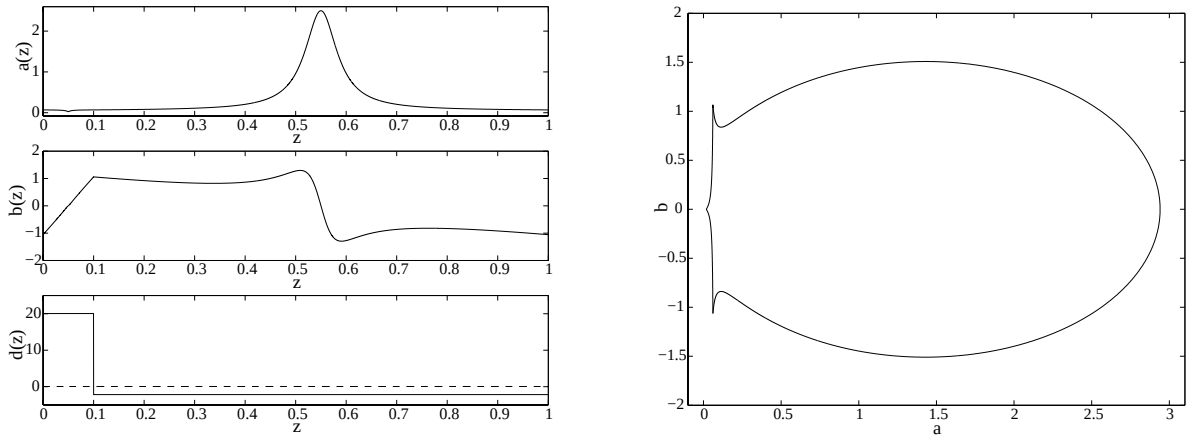

Fig. 1. Numerical approximation of the periodic solution $a(z)$ and $b(z)$ on $0 < z < 1$ with the parameters $l = 0.1$, $d_0 = 0.04$, $\alpha = 0$, and $E = 100$. Left: $a(z)$, $b(z)$ and the dispersion map $d(z)$. Right: Phase plane (a, b).

We now analyze the asymptotic solutions of system (2.5) in the limit of large pulse energy E. We shall work independently in two separate regions: $0 < z < l$ and $l < z < 1$, where $d(z) = d_0 + d_+ > 0$ and $d(z) = d_0 + d_- < 0$, respectively. Let $\epsilon = 1/E$ be a small parameter. We define new variables $\zeta_\pm$ in the two regions as

$$\epsilon \zeta_\pm = \int_{z_\pm}^{z} \gamma(z')dz', \tag{3.1}$$

where the values $z_\pm$ are defined to be the points on the focusing and defocusing fibers, where $b(z_\pm) = 0$. It follows from (2.5) that $a(z_\pm)$ has an extremum if $b(z_\pm)$ has a simple zero (cf. Figure 1). The transformation (3.1) is invertible since $\gamma(z) > 0$, i.e., the function $\zeta_\pm = \epsilon^{-1} g_\pm(z)$ is one-to-one with the inverse function $z = f_\pm(\epsilon\zeta_\pm)$. It is also clear from (3.1) that $\zeta_\pm = 0$ at the points, where $z = z_\pm$.

In new variables $\zeta_\pm$, the system (2.5) takes the form

$$\left\{ \begin{array}{rcl} \dfrac{da}{d\zeta_\pm} & = & \dfrac{a^{5/2} b}{(a^2+b^2)^{3/2}}, \\ \dfrac{db}{d\zeta_\pm} & = & \epsilon D(\epsilon\zeta_\pm) - \dfrac{a^{3/2}(a^2-b^2)}{2(a^2+b^2)^{3/2}}, \end{array} \right. \tag{3.2}$$

where

$$D(\epsilon\zeta_\pm) = \left. \frac{d(z)}{\gamma(z)} \right|_{z=f_\pm(\epsilon\zeta_\pm)}.$$

The system (3.2) can be reduced to the Hamiltonian form [6] with the $\zeta_\pm$-dependent Hamiltonians,

$$H(\zeta_\pm) = \frac{a^{1/2}}{(a^2+b^2)^{1/2}} - \frac{\epsilon D(\epsilon\zeta_\pm)}{a}. \tag{3.3}$$

We conclude from Figure 1 that the periodic solution $a(z)$ is centered and localized at the points $z = z_\pm$, where $\zeta_\pm = 0$. In the asymptotic region where $\zeta_\pm \sim \mathrm{O}(1)$ in the limit $\epsilon \to 0$, we expand $D(\epsilon\zeta_\pm)$ in a power series in ϵ at $\epsilon = 0$. Each partial system (3.2) becomes autonomous in the first order of ϵ with the following relation between a and b:

$$b^2 = \frac{a - \left(H_\pm a + \epsilon D_\pm\right)^2}{\left(H_\pm a + \epsilon D_\pm\right)^2} a^2, \tag{3.4}$$

where $H_\pm = H(0)$ and $D_\pm = D(0)$ are defined separately for the two regions of $\zeta_\pm$. The solution is defined in the domain $a^\pm_{\min} \le a(\zeta_\pm) \le a^\pm_{\max}$, where $a^\pm_{\min}$ and $a^\pm_{\max}$ are two roots of the quadratic equation

$$a = \left(H_\pm a + \epsilon D_\pm\right)^2. \tag{3.5}$$

We consider first the focusing fiber, where $D_+ > 0$. As follows from (2.7), the minimal value $a^+_{\min} = \min\limits_{0<z<l} a(z)$ is related to the map strength as $S = \frac{1}{a^+_{\min}}$. Under the condition that $H_+ = \mathrm{O}(\epsilon^p)$ with $p > -1$ in the limit $\epsilon \to 0$, one can expand the smallest root of the quadratic equation (3.5) in the power series of ϵ and find the leading-order expansion as

$$a^+_{\min} = \epsilon^2 D_+^2 \left(1 + \mathrm{O}(\epsilon H_+)\right). \tag{3.6}$$

We prove below that $H_+ = \mathrm{O}(\epsilon^{1/3})$ for $\alpha = 0$ and $H_+ = \mathrm{O}(1)$ for $\alpha \neq 0$, i.e., either $p = 1/3$ or $p = 0$, and the condition of validity of the leading-order approximation (3.6) is thus satisfied. In this case, the minimum of the peak of $a(\zeta_+)$ in the focusing fiber is $a^+_{\min} = \epsilon^2 A_{\min}$, where $A_{\min} = \mathrm{O}(1)$ in the limit $\epsilon \to 0$.

In the domain, where $\zeta_+ = \mathrm{O}(1)$ and $a(\zeta_+) = \epsilon^2 A_{\min} + \mathrm{O}(\epsilon^3)$, the system (3.2) has the leading-order asymptotic solution:

$$a(\zeta_+) = \epsilon^2 A_{\min} + \epsilon^3 A^2_{\min} \left(\frac{1}{\epsilon A_{\min}} - \frac{1}{\left(\epsilon^2 A^2_{\min} + D_+^2 \zeta_+^2\right)^{1/2}} \right) + R^+_a(\zeta_+, \epsilon), \tag{3.7}$$

and

$$b(\zeta_+) = \epsilon D_+ \zeta_+ + \frac{1}{2}\epsilon^2 D'(0)\zeta_+^2$$

$$+ \frac{1}{2}\epsilon^2 A_{\min}\left(\log\frac{D_+\zeta_+ + \left(\epsilon^2 A_{\min}^2 + D_+^2\zeta_+^2\right)^{1/2}}{\epsilon A_{\min}} - \frac{2D_+\zeta_+}{(\epsilon^2 A_{\min}^2 + D_+^2\zeta_+^2)^{1/2}}\right) + R_b^+(\zeta_+,\epsilon), \quad (3.8)$$

where the remainder terms have the order $R_a^+(\zeta_+,\epsilon) = \mathrm{O}(\epsilon^4)$ and $R_b^+(\zeta_+,\epsilon) = \mathrm{O}(\epsilon^3)$ in the region, where $\zeta_+ = \mathrm{O}(1)$. Comparison of the leading-order asymptotic solutions (3.7) and (3.8) (dashed curve) with the numerical approximation (solid curve) is shown on Figure 2 for the same values of parameters as on Figure 1.

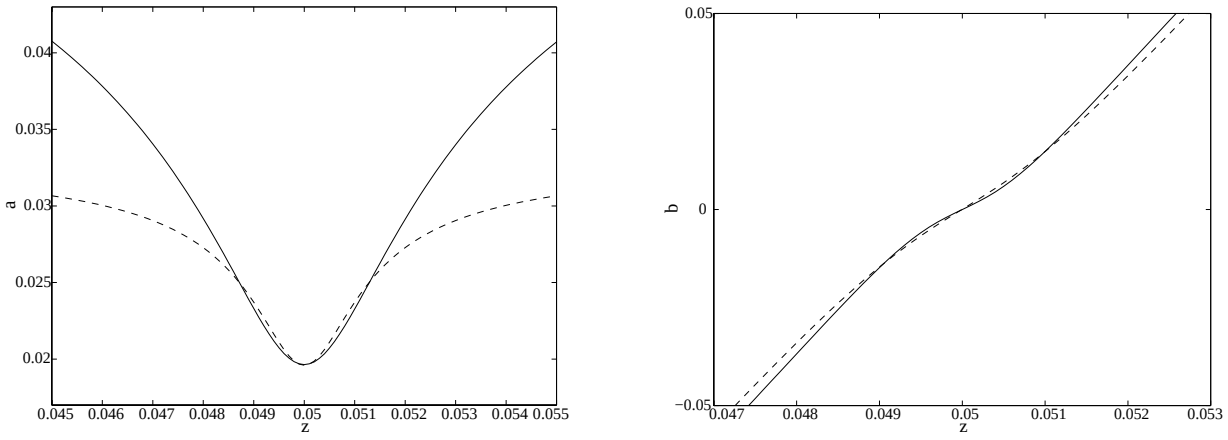

Fig. 2. Comparison of the numerical solution (solid curves) with the leading-order asymptotic solution (3.7) and (3.8). Left: $a(z)$. Right: $b(z)$.

The function $b(\zeta_+)$ grows secularly in the limits $\zeta_+ \to \pm\infty$, where the "inner" asymptotic approximation (3.8) breaks. It also follows from Figure 2 that the maximum of the function $a(\zeta_+)$ in the limits $\zeta_+ \to \pm\infty$ appears beyond the "inner" asymptotic approximation (3.7), where $a(\zeta_+) = \mathrm{O}(\epsilon^2)$. As a result, the asymptotic solutions $a(\zeta_+)$ and $b(\zeta_+)$ in (3.7)–(3.8) are not uniformly valid in the limit $\epsilon \to 0$ on $\zeta_+ \in \mathbb{R}$. The "inner" asymptotic solutions (3.7) and (3.8) must be matched with the "outer" asymptotic solution in the limits $\zeta_+ \to \pm\infty$ such that $\epsilon\zeta_+ \sim \mathrm{O}(1)$. The scaling of the system (3.2) with $b = \mathrm{O}(1)$ and $\epsilon\zeta_+ = \mathrm{O}(1)$ shows that the matching conditions are

$$\lim_{\substack{\zeta_+\to\pm\infty \\ \epsilon\zeta_+ = Z_\pm}} a(\zeta_+) = \epsilon^{2/3} A(Z_\pm), \qquad \lim_{\substack{\zeta_+\to\pm\infty \\ \epsilon\zeta_+ = Z_\pm}} b(\zeta_+) = B(Z_\pm). \quad (3.9)$$

The "outer" asymptotic solution $A(Z_\pm)$ and $B(Z_\pm)$ in the two limits satisfies the system of equations,

$$\begin{cases} \dfrac{dA}{dZ_\pm} &= \dfrac{A^{5/2}B}{(B^2+\epsilon^{4/3}A^2)^{3/2}}, \\ \dfrac{dB}{dZ_\pm} &= D(Z_\pm) + \dfrac{A^{3/2}(B^2-\epsilon^{4/3}A^2)}{2(B^2+\epsilon^{4/3}A^2)^{3/2}}. \end{cases} \quad (3.10)$$

We do not solve here the "outer" asymptotic system (3.10), but we exploit the scaling properties of the "outer" asymptotic solution (3.9). Since $D(Z_\pm)$ is independent of ϵ, it is clear from (3.3) that $H(\zeta_+)$ has the following representation at the "outer" asymptotic scale $\epsilon\zeta_+ = \mathrm{O}(1)$ in the limits $\zeta_+ \to \pm\infty$:

$$H(Z_\pm) = \epsilon^{1/3}\left(\frac{A^{1/2}}{(B^2+\epsilon^{4/3}A^2)^{1/2}} - \frac{D(Z_\pm)}{A}\right), \tag{3.11}$$

and therefore $H(Z_\pm) = \mathrm{O}(\epsilon^{1/3})$ as $\epsilon \to 0$. Since H is the Hamiltonian for the system (3.2), we have

$$\frac{dH}{d\zeta_+} = \frac{\partial H}{\partial \zeta_+} = -\frac{\epsilon^2 D'(\epsilon\zeta_+)}{a(\zeta_+)} = \frac{\epsilon^2}{a(\zeta_+)}\frac{d(z)\gamma'(z)}{\gamma^3(z)}\Big|_{z=f_+(\epsilon\zeta_+)}. \tag{3.12}$$

If $\gamma'(z) = 0$ (i.e., $\alpha = 0$) and $d(z) = d_0 + d_+ > 0$ in the focusing fiber $0 < z < l$, then

$$H(Z_\pm) = \lim_{\substack{\zeta_+\to\pm\infty \\ \epsilon\zeta_+ = Z_\pm}} H(\zeta_+) = H(0) = H_+, \tag{3.13}$$

and $H_+ = \mathrm{O}(\epsilon^{1/3})$ for $\alpha = 0$, as we claimed. If $\gamma'(z) \neq 0$ (i.e., $\alpha \neq 0$), then

$$H(Z_\pm) = H_+ + \epsilon^2 \int_0^{C_\pm} \frac{d\zeta_+}{a(\zeta_+)}\frac{d(z)\gamma'(z)}{\gamma^3(z)}\Big|_{z=f_+(\epsilon\zeta_+)} + \epsilon^2 \lim_{\substack{\zeta_+\to\pm\infty \\ \epsilon\zeta_+ = Z_\pm}} \int_{C_\pm}^{\zeta_+} \frac{d\zeta_+}{a(\zeta_+)}\frac{d(z)\gamma'(z)}{\gamma^3(z)}\Big|_{z=f_+(\epsilon\zeta_+)}, \tag{3.14}$$

where $C_\pm = \mathrm{O}(1)$ as $\epsilon \to 0$. The first integral in (3.14) is estimated with the "inner" asymptotic solution (3.7), where $a(\zeta_+) = \mathrm{O}(\epsilon^2)$, and the second summand in (3.14) is of order $\mathrm{O}(1)$ as $\epsilon \to 0$. The second integral in (3.14) is estimated with the "outer" asymptotic solution (3.9), where $a(\zeta_+) = \mathrm{O}(\epsilon^{2/3})$, and the third summand in (3.14) is of order $\mathrm{O}(\epsilon^{1/3})$ as $\epsilon \to 0$. As a result, $H_+ = \mathrm{O}(1)$ for $\alpha \neq 0$, as we claimed.

We consider next the defocusing fiber, where $D_- < 0$. Under the condition that $H_- = \mathrm{O}(\epsilon^q)$ for $q > -1$ in the limit $\epsilon \to 0$, one can expand the largest root of the quadratic equation (3.5) in the power series of ϵ and find the leading-order expansion as:

$$a^-_{\max} = \frac{1}{H_-^2}\left(1 + \mathrm{O}(\epsilon H_-)\right). \tag{3.15}$$

We show below that $H_- = \mathrm{O}(\epsilon^{1/3})$ for any value of $\alpha \geq 0$. In this case, the asymptotic expansion for the maximum of the peak of $a(\zeta_-)$ in the defocusing fiber is $a^-_{\max} = \epsilon^{-2/3}A_{\max}$, where $A_{\max} = \mathrm{O}(1)$ in the limit $\epsilon \to 0$. The scaling of system (3.2) with $a = \mathrm{O}(\epsilon^{-2/3})$ shows that the "inner" asymptotic solution on the defocusing fiber takes the form: $a(\zeta_-) = \epsilon^{-2/3}a(\eta_-, \epsilon)$, $b(\zeta_-) = \epsilon^{-2/3}b(\eta_-, \epsilon)$, where $\eta_- = \epsilon^{1/3}\zeta_-$. The leading-order "inner" asymptotic solution for $a(\zeta_-)$ and $b(\zeta_-)$ takes the explicit form:

$$a(\zeta_-) = \frac{4A^2_{\max}}{\epsilon^{2/3}\left(4A_{\max} + \eta_-^2\right)} + R_a^-(\eta_-, \epsilon), \tag{3.16}$$

and

$$b(\zeta_-) = -\frac{2\eta_- A^{3/2}_{\max}}{\epsilon^{2/3}(4A_{\max} + \eta_-^2)} + R_b^-(\eta_-, \epsilon), \tag{3.17}$$

where the remainder terms have the order $R_a^-(\eta_-, \epsilon) = \mathrm{O}(\epsilon^{2/3})$ and $R_b^-(\eta_-, \epsilon) = \mathrm{O}(\epsilon^{2/3})$ in the region, where $\eta_- = \mathrm{O}(1)$. The leading-order asymptotic solutions (3.16) and (3.17) (dashed curve)

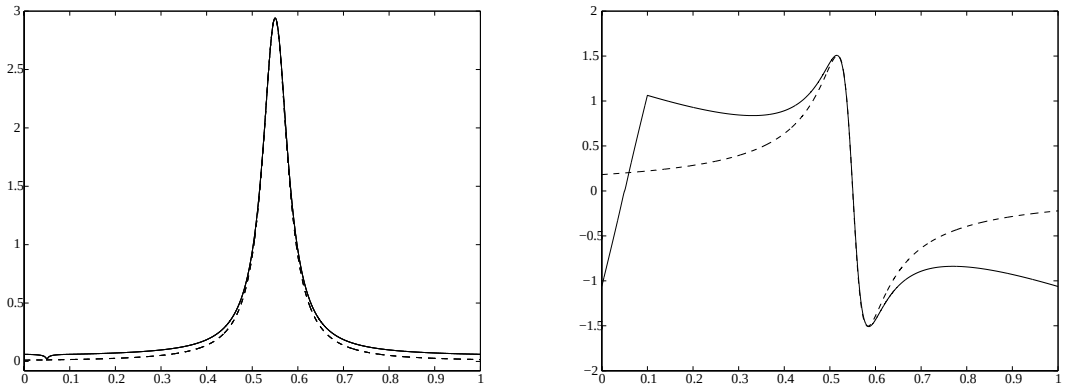

Fig. 3. Comparison of the numerical solution (solid curves) with the leading-order asymptotic solution (3.16) and (3.17). Left: $a(z)$. Right: $b(z)$.

are compared with the numerical approximation (solid curve) on Figure 3 for the same values of parameters as on Figure 1.

The asymptotic solutions $a(\zeta_-)$ and $b(\zeta_-)$ in (3.16)–(3.17) are not uniformly valid in the limit $\epsilon \to 0$ on $\zeta_- \in \mathbb{R}$. The "inner" asymptotic solutions (3.16) and (3.17) must be matched with the "outer" asymptotic solution in the limits $\zeta_- \to \pm\infty$, such that $\epsilon\zeta_- = \mathrm{O}(1)$. The matching conditions take the form

$$\lim_{\substack{\zeta_- \to \mp\infty \\ \epsilon\zeta_- = Z_\pm}} a(\zeta_-) = \epsilon^{2/3} A(Z_\pm), \qquad \lim_{\substack{\zeta_- \to \mp\infty \\ \epsilon\zeta_- = Z_\pm}} b(\zeta_-) = B(Z_\pm), \tag{3.18}$$

where the functions $A(Z_\pm)$ and $B(Z_\pm)$ are the same as in (3.9). The functions $A(Z_\pm)$ and $B(Z_\pm)$ solve the same problem (3.10), which is valid at the interface layer between the focusing and defocusing fiber, where $D(Z_\pm)$ changes sign. Since $D(Z_\pm)$ is independent of ϵ, the Hamiltonian $H(\zeta_-)$ has the same representation (3.11) with $D(Z_\pm) < 0$, and therefore $H(Z_\pm) = \mathrm{O}(\epsilon^{1/3})$ as $\epsilon \to 0$. Similarly to the focusing case, we find from (3.2) and (3.3) that

$$H(Z_\pm) = H_- + \epsilon^2 \lim_{\substack{\zeta_- \to \mp\infty \\ \epsilon\zeta_- = Z_\pm}} \int_0^{\zeta_-} \frac{d\zeta_-}{a(\zeta_-)} \frac{d(z)\gamma'(z)}{\gamma^3(z)}\Big|_{z=f_-(\epsilon\zeta_-)}, \tag{3.19}$$

where $d(z) = d_0 + d_- < 0$ in the defocusing fiber $l < z < 1$. Since $\epsilon^{2/3} A(Z_\pm) \le a(\zeta_-) \le \epsilon^{-2/3} A_{\max}$, the second term in (3.19) always has the order $\mathrm{O}(\epsilon^{1/3})$, such that $H_- = \mathrm{O}(\epsilon^{1/3})$ in the limit $\epsilon \to 0$, as we claimed. Thus, the asymptotic solution for $a(z)$ and $b(z)$ on a period $0 \le z \le 1$ is constructed with the help of the "inner" asymptotic solutions (3.7) and (3.8) in the focusing fiber, the "inner" asymptotic solutions (3.16) and (3.17) in the defocusing fiber, and the "outer" asymptotic solutions $A(Z_\pm)$ and $B(Z_\pm)$ of the interface problem (3.10) that match the "inner" solutions with the matching conditions (3.9).

The main result of the paper is the expansion (3.6), which gives the leading-order relation between the energy E and the map strength S as

$$E \sim D_+ \sqrt{S}. \tag{3.20}$$

We confirm this result with numerical approximations of the periodic solutions of system (2.5) for the case $l = 0.8$, $d_0 = 0.04$, and $\alpha = 0$. We first compute an approximate periodic solution for

small values of E, such as $E = 1$. The calculation is then repeated with increasing values for the pulse energy E and the map strength S. The numerical approximation of the curve E versus S is shown in Figure 4 (dashed curve), together with the asymptotic approximation (3.20) with $D_+ = d(l/2) = 2.54$ (solid curve).

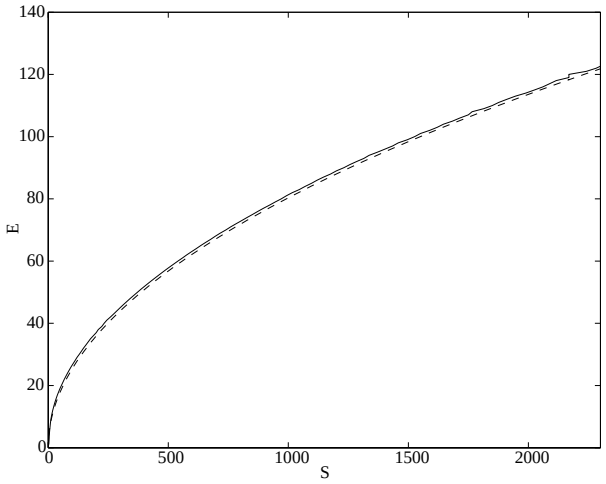

Fig. 4. Pulse energy E versus map strength S for $l = 0.8$, $d_0 = 0.04$, and $\alpha = 0$. Solid curve: numerical approximation, dashed curve: asymptotic approximation $E = D_+ S^{1/2}$.

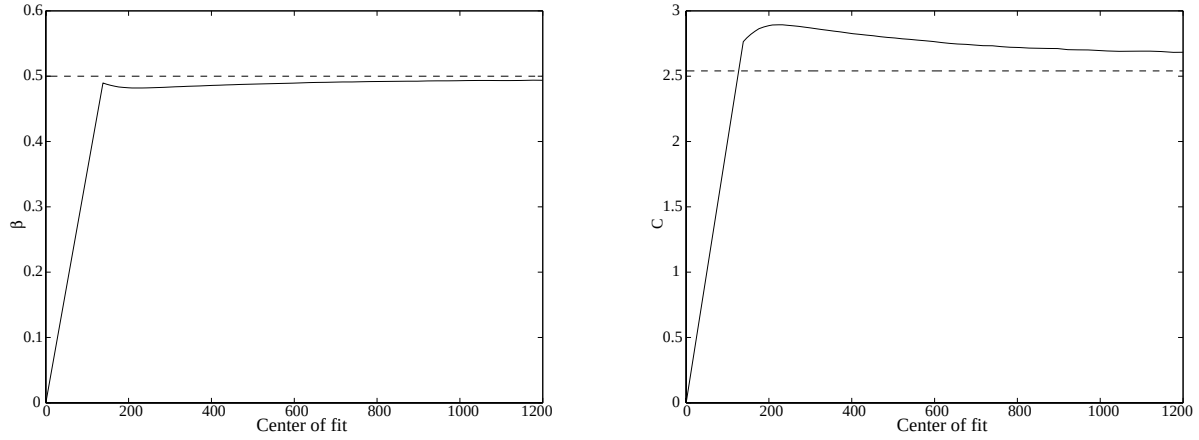

Fig. 5. Numerical approximations of parameters of the power regression fit $E = CS^\beta$. Left: β. Right: C. The center of the fit is taken at different values of S. The parameters are $l = 0.8$, $d_0 = 0.04$, and $\alpha = 0$, and the data are computed for $100 < E < 500$. Dashed lines show asymptotic results: $\beta = 0.5$ and $C = D_+$.

We apply the curve fitting algorithm for the power approximation $E = CS^\beta$ to 100 data points of the plot of E versus S, centered at a certain value of S. The power regression fit is shown in Figure 5 for different values of the center of the power fit in S. As the center of the power fit becomes larger, the computed value of constant C approaches $D_+ = d(l/2) = 2.54$ and the power β tends to 0.5. This confirms the leading-order asymptotic result (3.20). The computations are repeated with different values of the parameter l, with similar results.

The numerical approximations of the periodic solutions of system (2.5) are also obtained in the presence of loss and amplifications. Figure 6 shows the periodic solutions for the case $l = 0.1$, $d_0 = 0.04$, $\alpha = 0.75$, $z_a = 0.15$, and $E = 100$. Note that the minimum of $a(z)$ on the focusing fiber and the maximum of $a(z)$ in the defocusing fiber do not occur at the centers of the respective fibers. The locations of these points are denoted by $z_\pm$.

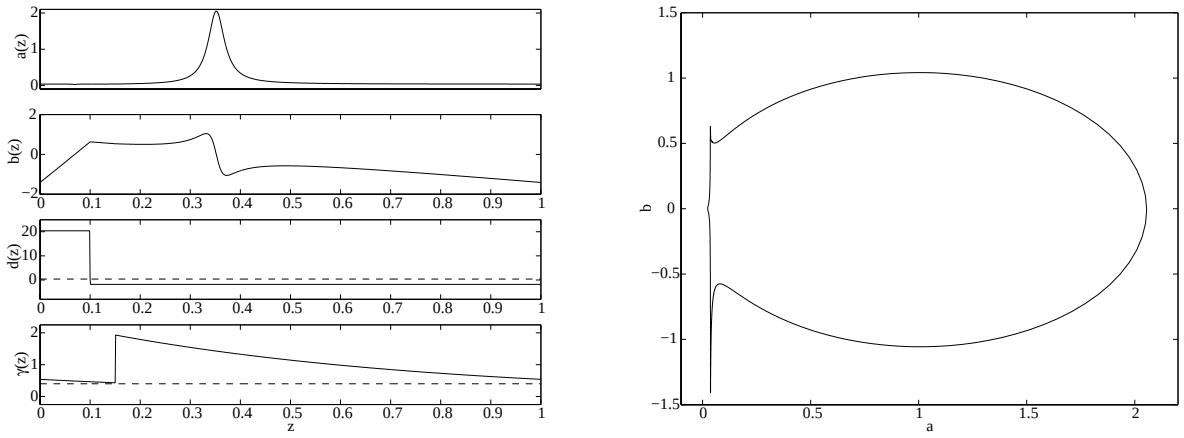

Fig. 6. Numerical approximation of the periodic solution $a(z)$ and $b(z)$ on $0 < z < 1$ in the presence of loss and amplification. The parameters are $l = 0.1$, $d_0 = 0.04$, $E = 100$, $z_a = 0.15$, and $\alpha = 0.75$. Left: $a(z)$, $b(z)$, dispersion map $d(z)$, and nonlinearity coefficient $\gamma(z)$. Right: Phase plane (a, b).

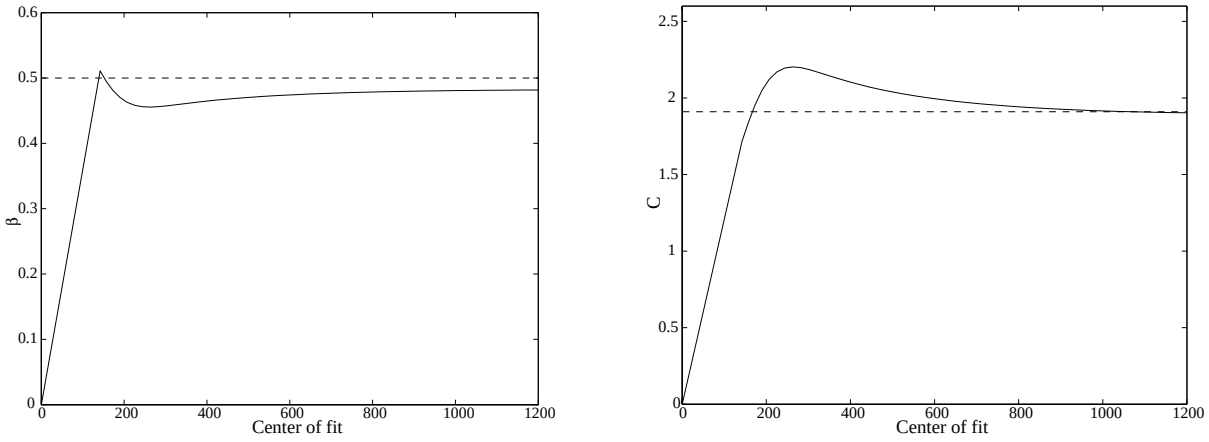

Fig. 7. Numerical approximations of parameters of the power regression fit $E = CS^\beta$ in the presence of loss and amplification. Left: β. Right: C. The center of the fit is taken at different values of S. The parameters are $l = 0.8$, $d_0 = 0.04$, $\alpha = 0.75$, and $z_a = 0.15$, and the data are computed for $100 < E < 500$. Dashed lines show asymptotic results: $\beta = 0.5$ and $C = D_+$.

The parameters β and C of the power fit $E = CS^\beta$ centered at different values of S are shown on Figure 7 for the case $l = 0.8$, $d_0 = 0.04$, $\alpha = 0.75$, and $z_a = 0.15$. As the center of the power fit becomes larger, the computed value of constant C approaches $D_+ = d(z_+)/\gamma(z_+) \approx 1.916$ and the power β tends to 0.5. This confirms the leading-order asymptotic result (3.20) in the case

when $\alpha \neq 0$.

4. SUMMARY

We have studied the relation between the energy E of dispersion-managed solitons and the map strength S of the dispersion map in the limit of large pulse energy. Using a matched asymptotic expansion, we have given leading-order expressions for the relation between E and S as well as for the functions a and b appearing in the dynamical system (2.5). The agreement between asymptotic and numerical results confirms our main claim that the pulse energy grows like $E \sim D_+\sqrt{S}$ with large map strength, where D_+ is the effective dispersion coefficient in the focusing fiber. The leading-order asymptotic solutions describe variations of the pulse parameters along the optical fiber. The delicate problems concerning the range of applicability of the asymptotic expansions and bounds on the error terms are relegated to future work.

REFERENCES

1. Kunze, M., Periodic Solutions of a Singular Lagrangian System Related to Dispersion-Managed Fiber Communication Devices, *Nonlinear Dynamics and Systems Theory*, 2001, vol. 1, pp. 159–167.
2. Kutz, J.N., Holmes, P., Evangelides, S.G., and Gordon, J.P., Hamiltonian Dynamics of Dispersion-Managed Breathers, *J. Opt. Soc. Am. B*, 1998, vol. 15, p. 87.
3. Lakoba, T.I. and Kaup, D.J., Hermite–Gaussian Expansion for Pulse Propagation in Strongly Dispersion-Managed Fibers, *Phys. Rev. E*, 1998, vol. 58, 6728.
4. Nakazawa, M., Kubota, H., Suzuki, K., Yamada, E., and Sahara, A., Recent Progress in Soliton Transmission Technology, *Chaos*, 2000, vol. 10, 486.
5. Pelinovsky, D., Instabilities of Dispersion-Managed Solitons in the Normal Dispersion Regime, *Phys. Rev. E*, 2000, vol. 62, 4283.
6. Pelinovsky, D. and Zharnitsky, V., Averaging of Dispersion-Managed Pulses: Existence and Stability, *SIAM J. Appl. Math.*, 2003, in press.
7. Turitsyn, S., Fedoruk, M.P., Shapiro, E.G., Mezentsev, V.K., and Turitsyna, E.G., Novel Approaches to Numerical Modeling of Periodic Dispersion-Managed Fiber Communication Systems, *IEEE J. Quantum Electr.*, 2000, vol. 6, p. 263.
8. Turitsyn, S.K. and Shapiro, E.G., Variational Approach to the Design of Optical Communication Systems with Dispersion Management, *Opt. Fiber Tech.*, 1998, vol. 4, pp. 151–188.